Leadership in Sustainable Infrastructure

Leadership en Infrastructures Durables

Vancouver, Canada

May 31 – June 3, 2017/ *Mai 31 – Juin 3, 2017*

INVESTIGATION OF SPATIAL AND TEMPORAL SEASONAL RAINFALL PATTERNS OVER SINAI PENINSULA

Elsanabary, Mohamed H.[1,4], Khafagy, Hadeer E.[2] and Abdellah, Sherif[3]

[1] Assistant Professor, Civil Engineering Department, Port Said University, Egypt

[2] Graduate Student, Civil Engineering Department, Port Said University, Egypt

[3] Associate Professor, Civil Engineering Department, Port Said University, Egypt

[4] mohamed.elsanabary@eng.psu.edu.eg

Abstract: Heavy rainfall events are one of the essential tough climate events especially in steep and mountainous regions with small drainage area such as Sinai Peninsula, Egypt, which can lead to devastating flash water causing massive damages to life and infrastructure. The main goal of this paper is to investigate rainfall spatial and temporal patterns over Sinai Peninsula for 1981 – 2015 and its teleconnection to El Niño region. This study employed the wavelet analysis and wavelet principal component analysis (WPCA) to analyze the seasonal rainfall gridded data over Sinai Peninsula. The paper focused on two seasons: from January to March (JFM) and the other from October to December (OND). Results showed that Sinai rainfall can be delineated into three zones: northern zone of Sinai bounded by the Mediterranean Sea and Suez Canal, the central plateau and the southern triangular zone between Suez and Aqaba gulfs. The study revealed that the dominant frequency of seasonal rainfall ranged between 2-4 years for both seasons. For (JFM) season, northern Sinai suffered from a serious decrease in rainfall from 1991 to 2005, whereas, the peaks of rainfall occurred during the periods 1981-1991 and 2005-2012. For (OND) season, southern Sinai witnessed rainfall decrease within the period 1981-1992, rainfall increase within the period 1993-2015. Moreover, the whole Peninsula was exposed to an abundance of rainfall in the period 1981-1992 and rainfall decrease from 1993-2015. Finally, the study found a strong teleconnection between El Niño region and the northern zone of Sinai, represented by El Arish city rainfall.

1 INTRODUCTION

Sinai Peninsula is the only part of Egypt located in Asia acting as a land bridge between Africa and Asia. In Sinai, the main activities of the Bedouin tribes are herding and rain cultivating (Elewa and Qaddah, 2011). Sinai Peninsula is characterized by steep and mountainous regions with small drainage area. For example, El Arish city is subjected to heavy rainfall events which can lead to devastating flash water causing massive damages to life and infrastructure. Therefore, studying rainfall spatial and temporal variability was a demand to reduce the impact of such events. Furthermore, rainfall Forecasting, using oceanic anomalies with a lead time, is very necessary to provide early warning before flash water events which in turn can minimize the resulting disasters. The mountainous nature of Sinai Peninsula and the war that hit the region for a long time making rainfall gauge data unavailable enough for rainfall forecasting. Previous studies, related to Sinai Peninsula rainfall, used hydrological and hydraulic models such as rainfall-runoff models to study flash flood risk in Sinai Peninsula considering the rainfall has a stationary characteristic such as (Cools et al. 2012; El-Sammany, 2010; Elsayyad et al., 2011; Masoud, 2009; Youssef et al., 2010; Abuzied et al., 2016). Cools et al. (2012) have developed an early warning

system (EWS) for flash floods for Wadi Watir, a part of Sinai Peninsula, based on field measurements, simulations, and remote sensing images. The results for 2010 flash flood show that 90% of the total rainfall volume was lost due to infiltration and transmission losses. Using the Weather Research and Forecasting Model (WRF), El-Sammany (2010) forecasted a total rainfall of 11.6 mm that cause a flash flood which took place over Wadi Watir, Sinai Peninsula, on October 24th, 2008 while the real measured one was 10.8 mm. El-Sammany (2010) showed significant consistency between WRF model and real measurements results. Some studies mapped flash flood risk using topographic, hydrological, and geological factors based on Rainfall-Runoff models. (Abuzied et al. 2016) assessed flash floods risk in the Nuweiba area located in Sinai Peninsula using soil Conservation Service (SCS) Rainfall-Runoff model then spatially integrated all the risk factors. Youssef et al. (2010) used GIS-based morphometry and satellite imagery to estimate the flash flood risk levels within the Wadi Feiran basin in Sinai Peninsula. Masoud (2009) analyzed the SRTM3 digital elevation model (DEM) and based on hydrologic characteristics and soil type during on-site visits, to derive morphometric parameters and the channel networks, in order to estimate flash flood of wadi catchments in Southern Sinai. Among previous studies, Elsayyad et al. (2011) investigated risk assessment of flash flood over Sinai Peninsula using similar techniques based on hydrological, metrological and hydraulic parameters.

This study takes into consideration the nonstationary variation of Sinai rainfall. Wavelet Principal Component Analysis (WPCA), a nonstationary technique, is applied to analyze the rainfall variability in space and time by applying the technique on rainfall gridded data of Sinai Peninsula. Elsanabary et al. (2014) applied wavelet Principal Component Analysis (WPCA), the non-stationary technique, to examine the spatial and temporal patterns of Ethiopian Highlands's rainfall. This paper performed wavelet principal component analysis (WPCA) for analyzing the nonstationary variations of Sinai Peninsula rainfall during the period (1981-2015) and define the spatial and temporal patterns. The main goal of this paper is to improve our understanding of the spatio-temporal rainfall variability over Sinai Peninsula, and find the teleconnection between such rainfall and El Niño region. The paper consists of six main sections. In section 2 the research objectives are shown, a brief description of the study area and rainfall data in section 3, the results and discussions in Section 5, and the summary and conclusions are given in Section 6.

2 RESEARCH OBJECTIVES

To meet the above goals, the objectives of this study are to employ the non-stationary technique of wavelet principal component analysis (WPCA) in order to investigate the non-stationary variation of Sinai seasonal rainfall for the two seasons (JFM) and (OND) from the period (1981-2015), Using the relations resulted to divide Sinai Peninsula into homogenous spatial patterns according to the nonstationary rainfall variability and determine the spatial localization of Sinai rainfall and investigate the periods of droughts, floods and their frequencies. Moreover, investigate the teleconnections between El Arish rainfall and climate anomalies such as El Niño.

3 STUDY AREA AND DATA

Sinai Peninsula is located in the northeastern part of Egypt and is bounded by longitudes 32°20′–34°52′E and latitudes 27°45′–31°10′N. It occupies an area of about 61,000 km^2 or about 6% of Egypt's total area with a population of about 400,000, which is mainly Bedouin (60%) and the rest are located in small cities such as El Arish and Sharm El Sheikh. The Peninsula has a triangular shape; its apex is to the south at Ras Mohammed (south of latitude 28°), whereas its base is to the north extending along the Mediterranean coast between Port Said and Rafah for about 210 km (Elewa et al., 2011). Sinai Peninsula is one of the coldest regions in Egypt because of its high altitudes and mountainous topography. Sinai Peninsula is characterized by two main rainy seasons. First one is from January to March (JFM) and the second is from October to December (OND). The rest of the year is dry. Precipitation data were collected for every year from October to March during the study period from 1981 to 2015. The data are monthly means of daily forecast accumulations. In order to have the whole Peninsula rainfall, another source of data was collected from ECWMF ERA-Interim dataset website at (http://apps.ecmwf.int/datasets/data/interim-mdfa/levtype=sfc/?). These data covers Sinai Peninsula over

(27.5°N-31.5°N) and (31.5°E-35.5°E) with grid resolution of (0.25° x 0.25°) from 1981 to 2015. Data contains 289 grid points. For verification of ERA- Interim dataset, gauge data were also collected from the Egyptian Meteorological Authority (EMA) for the period (2006 – 2015) for four gauge stations which are; Beer Elabd station at (30.59°N, 32.41°E), Al Melez station at (30.26°N, 33.10°E), El Arish station at (31.07°N, 33.46°E) and Sharm El_Sheikh station at (27.55°N, 34.19°E) as shown in Figure 1. Wars and Political conditions of Sinai Peninsula made gauge data of Sinai Peninsula rainfall isn't available enough to make a Long-term study and difficult to forecast the rainfall occurrence. The gauge data from the EMA was compared with ECMWF ERA-Interim gridded data, used in the study, in order to evaluate its reliability. Data comparison between the gridded data from ECWMF dataset and gauge data from EMA showed high correlation of 60% between El Arish station and gridded data at point (31°N, 33.50°E) with location difference of (-0.07°N, +0.04°E), high correlation (82%) between Sharm El_Sheikh station and gridded data at point (27.50°N, 34.25°E) with location difference of (-0.05°N, +0.06°E), medium correlation (50%) between Al Melez station and gridded data at point (30.25°N, 33°E) with location difference of (-0.01°N, -0.1°E) and low correlation (16%) between the last station Beer Elabd and gridded data at (30.50°N, 32.50°E) with location difference of (-0.09°N, +0.09°E), see Figure 2. The purpose of making this correlation is to investigate conformity of gridded data that will be used in the study with real gauge data. In order to confirm the teleconnection between Sinai rainfall and El Niño anomaly, El Niño SSTs data were downloaded from climate prediction center NOAA dataset at (http://www.cpc.ncep.noaa.gov/data/indices/oni.ascii.txt).

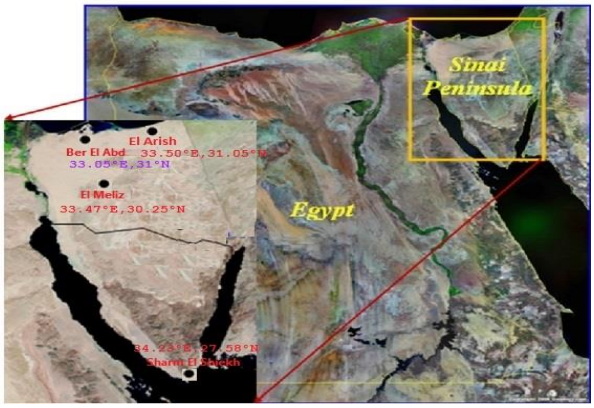

Figure 1: Sinai Peninsula's map showing the locations of four gauge stations of monthly rainfall data from EMA used in this study

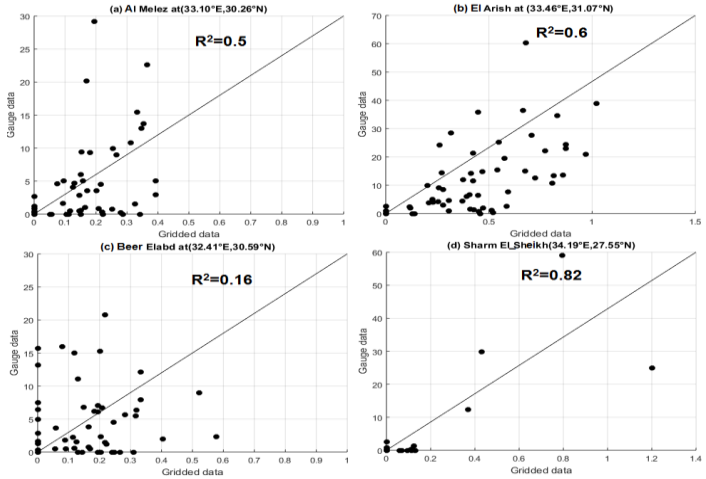

Figure 2: correlation between gridded data from ECWMF dataset and gauge data from EMA at four stations (a) Al Melez station, (b) El Arish station, (c) Beer Elabd station and (d) Sharm El_Sheikh station

4 METHODOLOGY

It is useful to have an idea about the possible techniques that can be used to identify spatial and temporal rainfall characteristics over the Sinai Peninsula. These possible techniques include Fourier Spectral Analysis, Hilbert-Huang transformation and Wavelet Analysis (WA). Fourier analysis technique considers the time series as a stationary time series while Hilbert-Huang transformation is suitable for analysing the nonlinear-nonstationary characteristics of rainfall. Considering the nonstationary variation of the rainfall over Sinai Peninsula, the nonstationary technique of Wavelet Analysis (WA) was used (Torrence and Compo 1998). WA is a mathematical means for performing signal analysis when signal frequency varies over time (Torrence and Compo 1998). Wavelet is convenient for studying nonstationary characteristics of any patterns such as rainfall (Elsanabary et al. 2014). The Morlet wavelet is a good choice because it is commonly used, simple and looks like the rainfall signals. Principal Components Analysis (PCA) is a way of identifying patterns in data and expressing the data in such a way to highlight their similarities and differences. The main advantage of PCA is compressing the data by reducing the number of dimensions without much loss of information. However, PCA method cannot eliminate out noise well enough. Therefore, a better solution is to combine wavelet analysis with PCA, called Wavelet PCA, which can improve the results. Wavelet power spectra and global wavelet spectra were used to define the prevalent frequency period. After that SAWP was calculated for each of the 289 rainfall grid points. Finally, Wavelet coherence was applied to El Arish gridded rainfall data and El Niño region to investigate the teleconnection between the two variables.

5 RESULTS

Wavelet and global spectra for all 289 grid points of the two seasons were calculated but couldn't be shown all. Figure 3(a) and Figure 3(b) show examples of wavelet and global spectra of Sinai rainfall at (33.5°E, 30.25°N) and (33.50°E, 30.75°N) respectively during the studying period 1981–2015 at OND season. The SAWP for rainfall was computed using the 2–4, 5-7 and 2-8 years frequency range. According to Figure 3 and other figures not shown, statistically significant power in JFM and OND Sinai rainfall was found to have occurred within the 2-8 years frequency band during the study period 1981–2015.

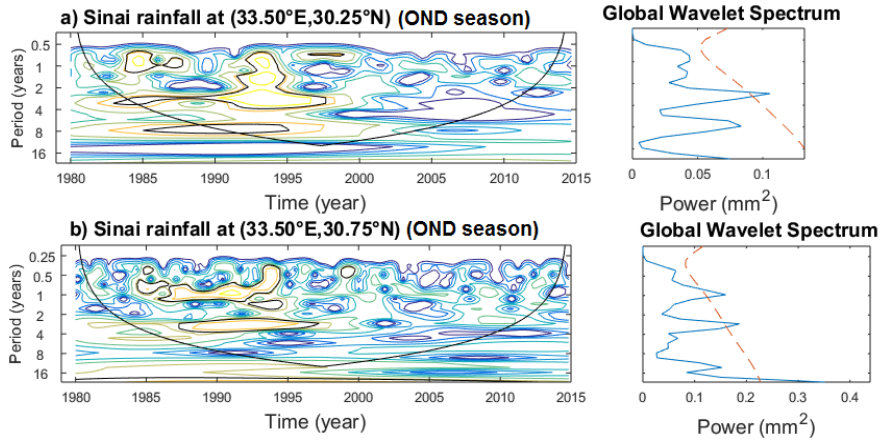

Figure 3: Examples of wavelet power spectra and global wavelet spectra plot at (a) (33.50°E, 30.25 °N) and (b) (33.50°E, 30.75°N)

To determine the dominant spatial and temporal characteristics of Sinai rainfall, wavelet principal component analysis (WPCA) was applied to the SAWP of rainfall (Elsanabary et al. 2014). Before applying PCA, all rainfall time series were standardized by subtracting the mean and then dividing by the standard deviation. Eigenvectors in principle component analysis provide us with information about the patterns in the data by extracting axes that characterize the data. In general, once eigenvectors are found from the covariance matrix, the next step is to order them by eigenvalues, highest to lowest. The

eigenvector with the highest eigenvalue is the principle component of the data set. When using a filtered time series, such as the SAWP, a useful way to determine the number of signals presented in a time series can be done by observing spatial patterns of the eigenvectors. The number of eigenvectors determines the number of signals which represent the time series and the discarded eigenvectors considered as noise. Figure 4 shows that Sinai rainfall seasons JFM and OND may have up to two distinct signals represented by two essential eigenvectors (i.e. the first and the second principal component) representing more than 97% of the total variance for January to March (JFM) season and 95% of the total variance for October to December (OND) season for 2-8 years frequency band. For 2-4 and 5-7 years frequency bands the first and the second principal component representing more than 93% and 98% respectively of the total variance for JFM season and more than 97% and 98% respectively of the total variance for OND season.

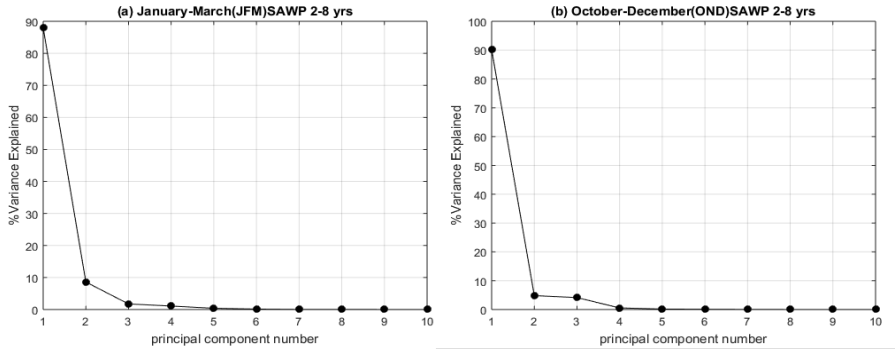

Figure 4: Scree plot of Sinai rainfall data of the first ten principal components which show that the first two principal components generally explain more than 97% of the total variance (a) for January to March and more than 95% of the total variance (b) for October to December for 2-8 years frequency band

5.1 Spatial patterns of Sinai rainfall

5.1.1 January to March (JFM) Rainfall

Figure 4 shows WPC1 and WPC2 accounted for, approximately, 97% of the rainfall variability where WPC1 and WPC2 explaining about 88% and 9% respectively for 2-8 years frequency band. For the analysis, 2-8 years frequency band was chosen as it is the most convenient for our data and is the same frequency of El Niño region. Figure 5 shows a topographic map of Sinai Peninsula that will be used to compare the rainfall patterns with the topography of the whole map. Figure 6 (a and b) display the correlation between each of the 289 grid point SAWP with WPC1 and WPC2 respectively for JFM season within the frequency band 2-8 years. According to figure 6 (a), WPC1 is positively correlated with SAWP for all the area of Sinai (all grid points) except the zero correlation found in the south western between (33.25°E-34°E) and (28°N-29°N). The strongest positive correlation was found in the eastern north overlooking the Mediterranean Sea between (33°E-34.5°E) and (30.25°N-31.25°N). The correlation decreases southwards towards the triangular part in the south. Figure 6 (b) describes the WPC2 correlation with SAWP where negative correlation was found in the majority of Sinai Peninsula except for the positive correlation in the western north area between (32.5°E-34°E) and (30°N-31°N) including one gauge station under study Al Melez at (30.26°N, 33.1°E). Figure 6 (a) appears more similar to figure 6 (e) than figure 6 (c) this clarifies that spatially 5–7 years frequency period is more dominant within the 2–8 years frequency band than the 2–4 years frequencies. Whereas, figure 6 (d) appears more similar to figure 6 (b) than figure 6 (f) showing that 2–4 years frequency period is more dominant within the 2–8 years frequency band than the 5–7 years frequencies.

The spatial correlation between SAWP with WPC1 and WPC2 for JFM season produced zones that are similar to that of the topographic contour map of the Sinai Peninsula that is shown in Figure 5. The rainfall over the southern region with elevated mountains of Sinai seems to have low correlation with WPC1. The hilly region in northern Sinai seems to have high positive correlation with WPC1. The central plateau

seems to range in positive correlation values descending southwards. Generally, rainfall seems to decrease southwards while the elevation of the terrain increases and vice versa.

According to the spatial patterns of the three frequency bands 2-8, 2-4 and 5-7 years Sinai's January to March (JFM) rainfall season rainfall can be delineated into three zones: northern zone of Sinai bounded by the Mediterranean Sea and Suez Canal, the central plateau and the southern triangular zone between Suez and Aqaba gulfs.

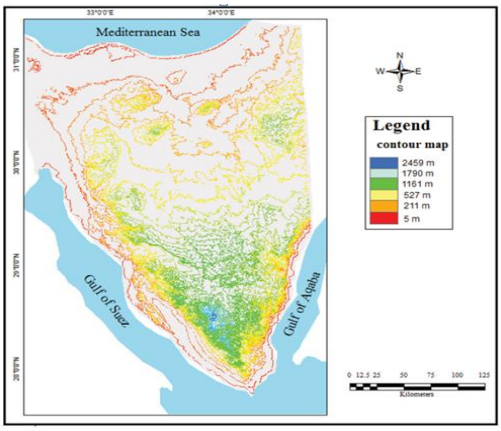

Figure 5: Topographic contour map showing land elevations in Sinai Peninsula from (Elsayyad et al. 2011)

5.1.2 October to December (OND) Rainfall

Figure 7 shows the correlation, between each of the 289 grid point SAWP with WPC1 and WPC2 for OND season. WPC1 (representing 90% of the gridded rainfall data)is positively correlated to SAWP for the total area of Sinai Peninsula within 2-8 years frequency band as shown in Figure 7 (a). While Figure 7 (b) shows that WPC2 (representing 5% of the gridded rainfall data) is negatively correlated to SAWP at almost all parts of the Sinai Peninsula, whereas it seems to be positively correlated to a small part of the northern coast of Sinai at 31°N-31.25°N and 34°E-34.5°E. Figure 7 (a) appears more similar to figure 7 (c) than figure 7 (e) and also figure 7 (d) appears more similar to figure 7 (b) than figure 7 (f). The results indicate that spatially 2–4 years frequency band is more dominant within the 2–8 years frequency band than the 5–7 years frequency band. Similarly, for the JFM rainfall season, the energy within the 2–4 years for OND rainfall season is dominating the rainfall over Sinai Peninsula.

There is similarity between results shown in figure 7 and the topographic map in Figure 5. Generally, the positive correlation between SAWP and WPCs, of OND season, decreases southward as the altitude increases and vice Versa. The 2-4 years frequency band WPC1 and WPC2 represents 91% and 6% of SAWP data respectively. Moreover, the 2-8 years frequency band WPC1 and WPC2 represents 90% and 5% of the data respectively. Generally, the spatial patterns of JFM and OND rainfall seasons divide Sinai Peninsula into three zones: northern zone of Sinai bounded by the Mediterranean Sea and Suez Canal, the central plateau and the southern triangular zone between Suez and Aqaba gulfs.

5.2 Temporal Patterns

5.2.1 JFM Rainfall

Figure 8 shows the temporal variations of the leading eigenvectors (i.e. WPC1 and WPC2) of Sinai Peninsula for JFM rainfall season based on 2–4, 2-8 and 5-7 years frequency bands. For JFM rainfall season, Figure 8 (a) shows a positive gradient in WPC1 that dominated northern Sinai Peninsula for the period 1981-1991 and 2005-2012. Sinai rainfall was in stagnation for the period 1991 to 2005 which appears as a negative gradient in WPC1. Generally, WPC1 varies with high energy from 1981 to 1991 and from 2005 to 2012. The highest rainfall values were in 1987, 1991 and 2012 whereas the least rainfall values were in 2000 and 2005. WPC1 is high positively correlated to northern Sinai within the JFM

rainfall, the variations in energy show that northern Sinai suffered from a serious decrease of rainfall for 1992-2005. On the other hand, there is an abundance of rainfall in the periods (1981 – 1991) and (2005 – 2012). Figure 8 (b) shows the temporal variations of WPC2 where rainfall increased slightly in (1981 – 1983), (1992 – 2003) and (2009 – 2013), while rainfall decreased in (1983 – 1991) and (2003 – 2009). Moreover, the rainfall peaks values were in 1983, 1998, 2003 and 2013 while the lowest rainfall values were in 1992 and 2009. WPC2 is highly negatively correlated with the southern triangular part of Sinai Peninsula. As a result, the southern triangular part of Sinai Peninsula was exposed to abundance periods of rainfall in (1983 – 1991) and (2003 – 2009). Also, the southern triangular part was exposed to rainfall decrease in (1981 – 1983), (1992 – 2003) and (2009 – 2013). For 2-8 years frequency band, WPC1 and WPC2 accounted for 97% of total rainfall variability where WPC1 and WPC2 explaining about 88% and 9% respectively. In Figure 8 (a), there is similar pattern of WPC1 for the 2 – 4 and 2-8 frequency bands during JFM season. WPC1 was largely dominated by the 2–4 years cycle rather than 5–7 years cycle, as well as WPC2 was dominated by 2 – 4 year cycle, see Figure 8 (b).

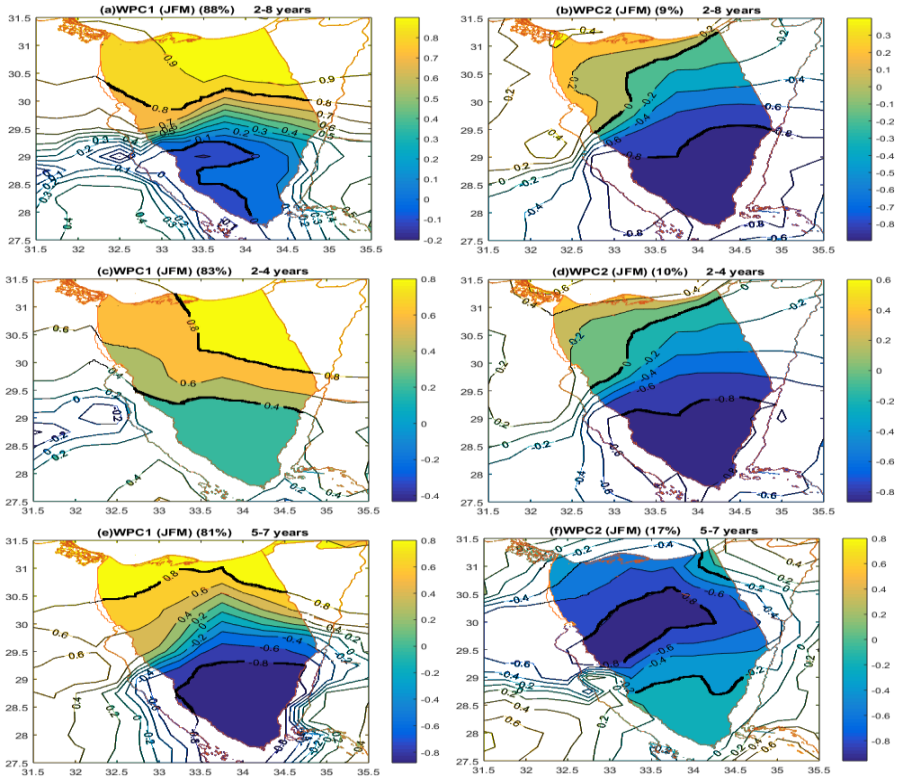

Figure 6: Spatial correlation of SAWP with WPC1 (a) 88% (c) 83% (e) 81% of gridded rainfall data within the frequency bands 2-8, 2-4 and 5-7 year respectively and with WPC2 (b) 9% (d) 10% (f) 17% of gridded Sinai rainfall data within the frequency bands 2-8, 2-4 and 5-7 year for JFM season respectively

5.2.2 OND Rainfall

According to Figure 9 when using 2–8, 2-4 and 5-7 year frequency bands to compute WPC1 and WPC2 at OND rainfall season. WPC1 shows a positive gradient in the period (1981-1992); see Figure 9 (a). Also, a negative gradient was observed in the rest of the study period (1992 – 2015). The rainfall peak was observed in in 1992. WPC1 is highly positive correlated with the majority of Sinai within the OND rainfall season. The variations in energy show that approximately, the total area of Sinai has an abundance of rainfall in the period (1981-1992) and rainfall decrease in (1993 – 2015) while WPC2 is highly negative correlated with the southern triangular area of Sinai Peninsula. Therefore, it suffered from rainfall decrease within the period of (1981 – 1992). Rainfall increases within the period of (1993 – 2015) and the decreases during 1992. For 2-4 year frequency band, WPC1 and WPC2 represent 91% and 6% respectively of SAWP data while for 2-8 year frequency band WPC1 and WPC2 represent 90% and 5%

of the data respectively. Comparing Figure 9 (a) and (b) we can notice that the frequency band 2-4 year within 2-8 years frequency band have a convenient representation of the data better than the 5-7 year frequency band for both WPC1 and WPC2.

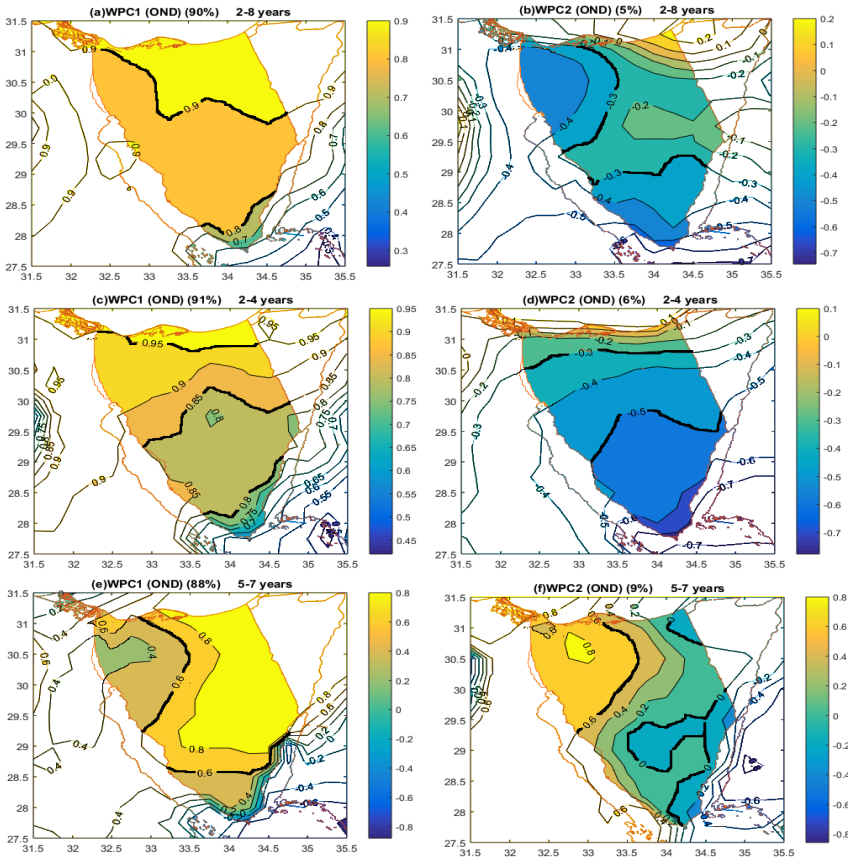

Figure 7: Spatial correlation between SAWP and WPC1 (a) 90% (c) 91% (e) 88% of gridded rainfall data within the frequency bands 2-8, 2-4 and 5-7 year respectively and between SAWP and WPC2 (b) 5% (d) 6% (f) 9% of gridded rainfall data within the frequency bands 2-8, 2-4 and 5-7 year for OND season respectively

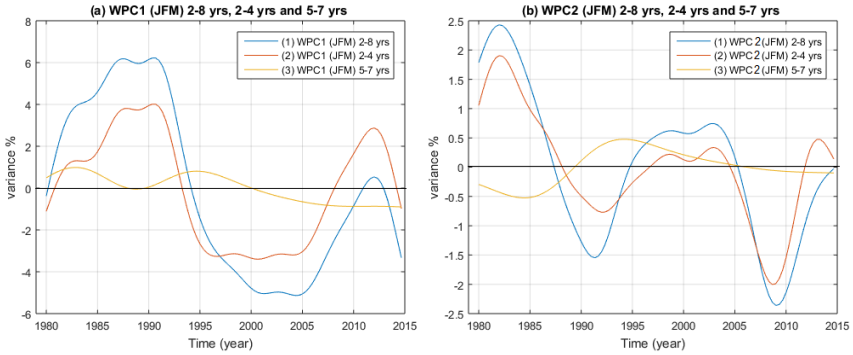

Figure 8: Time series of (a) WPC1 and (b) WPC2 of Sinai January to March (JFM) rainfall season computed using 2–8, 2-4 and 5-7 year frequency bands.

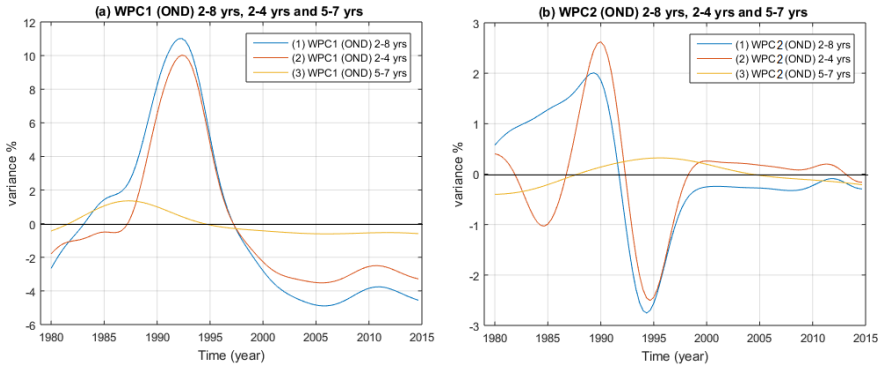

Figure 9: Time series of (a) WPC1 and (b) WPC2 of Sinai October to December (OND) rainfall season computed using 2–8, 2-4 and 5-7 year frequency bands.

5.3 Coherence between El Arish rainfall and El Niño

To understand the correlation between El Niño region and El Arish rainfall, the 3-month lead time, the July-September (JAS) and OND El Niño anomalies were used to help with forecasting of OND and JFM El Arish rainfall respectively. The association was assumed to exist if the temporal variation of the El Niño and rainfall were well correlated (Mwale et al. 2007). Figure 10(a) shows the wavelet coherence between El Arish (JFM) rainfall and El Niño (OND). The coherence between El Arish (JFM) rainfall and El Niño (OND) remains stable for the period 1990 to 1998. The rainfall over El Arish (JFM) shows an inter-annual coherence of over 0.8 with El Niño (OND) for the period 1998-2010. It seems that El Niño (OND) SST is leading the significant coherence. Figure 10(b) shows the wavelet coherence between El Arish (OND) rainfall and El Niño (JAS) SST. There is in phase relationship between El Niño (JAS) and El Arish (OND) rainfall for time periods of significant coherence from 1995 to 2010.

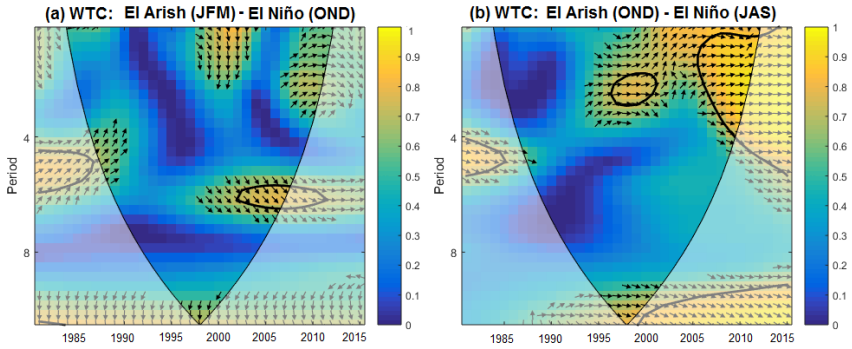

Figure 10: Wavelet Coherence between (a) El Arish (JFM) rainfall and El Niño (OND) SST (b) El Arish (OND) rainfall and El Niño (JAS) SST

6 SUMMARY AND CONCLUSIONS

This paper discusses the spatial and temporal seasonal rainfall characteristics over the Sinai Peninsula during two rainy seasons including January to March (JFM) season and October to December (OND) season. Non-stationary analysis technique was employed by applying wavelet analysis and WPCA on gridded rainfall data of the Sinai Peninsula in order to analyze the variability of rainfall in space and time due to the non-stationary variation of rainfall. These techniques were also applied to El Niño anomaly to teleconnect Sinai rainfall and El Niño region. According to the study, Sinai Peninsula was delineated into three zones: northern zone of Sinai bounded by the Mediterranean Sea and Suez Canal, the central plateau and the southern triangular zone between Suez and Aqaba gulfs. Temporal characteristics of the leading WPC signals showed that northern Sinai within the (JFM) rainfall season had been in stagnation in the period from 1991 to 2005, the peaks of rainfall occurred during the periods 1981-1991 and 2005-2012 while southern Sinai (OND) rainfall season

witnesses rainfall decrease in 1981-1992. The dominant frequency in Sinai rainfall ranged between 2 and 8 years. By examining both (5-7years) and (2- 4years) frequency regimes to understand rainfall nonstationary, dominated behavior seems to be (2- 4years) frequency band. The teleconnection between El Niño region and El Arish rainfall was found by applying Wavelet Coherence between El Arish (JFM) and (OND) rainfall and El Niño (OND) and (JAS) respectively. This will help in forecasting floods and droughts over El Arish city.

7 ACKNOWLEDGEMENTS

The authors would like to thank the Egyptian Meteorological Authority for providing the gauge data of the four rainfall gauges used in the study.

8 REFERENCES

Abuzied, Sara, May Yuan, Samia Ibrahim, Mona Kaiser, and Tarek Saleem. "Geospatial risk assessment of flash floods in Nuweiba area, Egypt." Journal of Arid Environments, 2016.

"A cross wavelet and wavelet coherence toolbox for MATLAB." Aslak Grinsted. Accessed April 20, 2017. http://www.glaciology.net/wavelet-coherence.

Climate Prediction Center. Accessed February 18, 2017. http://www.cpc.ncep.noaa.gov/data/indices/oni.ascii.txt.

Cools, J., P. Vanderkimpen, G. El Afandi, A. Abdelkhalek, S. Fockedey, M. El Sammany, G. Abdallah, M. El Bihery, W. Bauwens, and M. Huygens. "An early warning system for flash floods in hyper-arid Egypt." Natural Hazards and Earth System Science , 2012.

Elewa, Hossam H., and Atef A. Qaddah. "Groundwater potentiality mapping in the Sinai Peninsula, Egypt, using remote sensing and GIS-watershed-based modeling." *Hydrogeology Journal*, 2011.

ERA-Interim, Monthly Means of Daily Forecast Accumulations. Accessed February 09, 2017. http://apps.ecmwf.int/datasets/data/interim-mdfa/levtype=sfc/.

El-Sammany, Moustafa. " Forecasting of Flash Floods over Wadi Watier – Sinai Peninsula Using the Weather Research and Forecasting (WRF) Model". World Academy of Science, Engineering and *Technology International Journal of Environmental, Chemical, Ecological, Geological and Geophysical Engineering*, 2010.

Elsanabary, Mohamed Helmy, Thian Yew Gan, and Davison Mwale. "Application of wavelet empirical orthogonal function analysis to investigate the nonstationary character of Ethiopian rainfall and its teleconnection to nonstationary global sea surface temperature variations for 1900-1998." *International Journal of Climatology*, 2014.

Elsanabary, Mohamed Helmy, and Thian Yew Gan. "Investigation of Seasonal Rainfall Variability over the Ethiopian Highlands: Teleconnection between the Upper Blue Nile Basin Rainfall and the Oceanic Anomalies." *Annual Conference of the Canadian Society for Civil Engineering*, 2012.

Elsayyad, Mohamed Ashraf, Gamal Ibrahim Kotb, Abd El-Moniem Sanad. "Risk assessment of flash flood in Sinai ". *Arab Academy For Science, technology and Maritime Transport,* 2011.

Masoud, Alaa A. "Runoff modeling of the wadi systems for estimating flash flood and groundwater recharge potential in Southern Sinai, Egypt." *Arabian Journal of Geosciences*, 2009.

Mwale, Davison, Thian Yew Gan, Samuel S. P. Shen, Ting Ting Shu, and Kyu-Myong Kim. "Wavelet Empirical Orthogonal Functions of Space-Time-Frequency Regimes and Predictability of Southern Africa Summer Rainfall." *Journal of Hydrologic Engineering*, 2007.

Torrence C, Compo GP. " A practical guide to wavelet analysis". *Bulletin of the American Meteorological Society*, 1998.

Youssef, Ahmed M., Biswajeet Pradhan, and Abdallah Mohamed Hassan. "Flash flood risk estimation along the St. Katherine road, southern Sinai, Egypt using GIS based morphometry and satellite imagery." *Environmental Earth Sciences*, 2010.